# The Technology of Crowd-Sourcing Landmarks-Assisted Smartphone in Indoor Localization

**XINXIN WANG[1], DANYANG QIN[1], (Member, IEEE), RUOLIN GUO[1], MIN ZHAO[1], LIN MA[2], (Member, IEEE), AND TEKLU MERHAWIT BERHANE[3]**

[1]School of Electronics Engineering, Heilongjiang University, Harbin 150080, China
[2]Harbin Institute of Technology, Harbin 150001, China
[3]School of Electrical and Computer Engineering, Dire Dawa University (DDU), Dire Dawa 1362, Ethiopia

Corresponding author: Danyang Qin (qindanyang@hlju.edu.cn)

**ABSTRACT** In recent years, with the popularity of smartphones, mobile sensor technologies have been widely used in indoor localization. Its advantage is that data can be collected directly from smartphones without installing any other equipment. Meanwhile, it has the disadvantages of high requirements on positioning conditions and large deviations in positioning results. A technology of crowd-sourcing landmarks-assisted smartphone in indoor localization (CLS-IL) is proposed in this paper so as to solve these disadvantages. Firstly, the accelerometer, magnetometer and gyroscope sensors are used to acquire initial positioning of users. The characteristics of magnetometer and gyroscope sensors are analyzed through a series of experiments in allusion to the key problem of heading estimation errors, then corresponding data is matched for different experimental conditions. After that, the corresponding landmark database is established for experimental environment and an adaptive optimization algorithm of landmarks is proposed to correct drift errors caused by the readings of sensors influenced by surrounding environment and long positioning time excessively during traditional pedestrian dead reckoning. Experimental results show that the location accuracy of CLS-IL system is significantly improved compared with traditional technologies, which provides strong support for subsequent studies.

**INDEX TERMS** Adaptive optimization, crowd-sourcing landmarks, indoor localization, mobile sensors, smartphones.

## I. INTRODUCTION

With the constant update and rapid development of mobile terminal devices and Internet technologies, the demand for location-based services (LBS) [1] is also increasing. In recent years, outdoor positioning technology has become more mature, global positioning system (GPS) with its efficiency, speed and accuracy has been able to meet people's needs of outdoor positioning and navigation. However, due to the complexity of indoor structures and the increase number of obstacles, signals are easily blocked and there are multipath effects [2] in indoor environment. Leading to the slow development of indoor positioning technology such as large railway stations, museums, shopping malls, attractions, etc.

The associate editor coordinating the review of this manuscript and approving it for publication was Miltiadis Lytras.

At the same time, the demand for indoor positioning becomes stronger as indoor environment becomes more complex and indoor activities become more frequent.

A lot of studies have been conducted in order to obtain accurate indoor positioning results. At present, indoor localization technologies that are widely used include wireless local area networks (WLAN) [3], visible light [4], ultra-broadband [5], Bluetooth [6], micro electro mechanical systems (MEMS) [7], infrared [8], computer vision [9], geomagnetic [10], radio frequency identification (RFID) [11] and other positioning technologies. The classification and research development of indoor positioning technologies are illustrated in Figure 1. It includes triangulation [12], trilateration [13], fingerprint technology [14], [15], simultaneous localization and mapping (SLAM) [16], [17] and crowdsourcing-based technology [18], [19], etc.
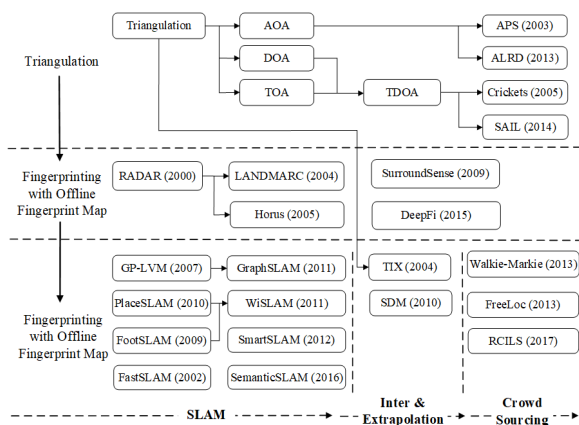
**FIGURE 1.** Classification of indoor positioning technologies.

However, many common indoor positioning technologies have their own shortcoming [20]. Such as infrared technology, it has high positioning accuracy, but the equipment is expensive and it is easily to be affected by environment. RFID technology needs to place a large number of equipment in positioning area which leading numerous tasks. Wireless Fidelity (Wi-Fi) is the common method in indoor positioning, but it has the disadvantage of large fluctuation of signal strength.

In recent years, with the rapid development of the smartphone industry, using built-in sensors of smartphones for positioning has become the most suitable indoor positioning method [21] and an important content of research in this field. It has the features of low cost and low complexity and it does not need to add additional equipment [22]. At the same time, it has the disadvantages of high requirements on the positioning environment and large deviations in positioning results. Because the readings of the built-in sensors of smartphones are easily affected by surrounding environment, it will cause problems such as directional deviations and drift errors [23]. And once an error occurs, the error will be accumulated continuously, so it will not be able to provide support for subsequent navigation applications.

In order to solve the problems of orientation errors and drift errors caused by built-in sensors of smartphones, this paper proposes an indoor localization technology based on landmark-assisted mobile sensors. Due to the limitations of using image visual positioning of smart mobile terminals in commercial supermarkets, airports, train stations, teaching buildings and other places (because of duplicate logos, similar scenes, etc.). Moreover, visual image landmarks are easily affected by light, angle and user's walking speed in surrounding environment, resulting in the fluctuation of detection results which lead to volatile results. Therefore, this paper uses low power Bluetooth beacon as landmark instead of traditional visual landmark. Low power Bluetooth has the advantages of easy deployment, low cost and low latency and most mobile devices are equipped with Bluetooth modules. Therefore, it can be used only with unique test software, without adding additional test equipment and

it is easy to implement and put into using. Beacons are small battery-powered devices that can continuously broadcast BLE signals to all devices that are listening. By applying the iBeacon [24] structure to beacons, the value of signal intensity can be easily identified, so they are favored in indoor positioning.

Errors of dead reckoning results are corrected by using landmarks to obtain accurate information of dead reckoning and user coordinates effectively, and reduce location error and convergence time. In addition, this system still has strong stability in airports, train stations with poor Wi-Fi network signals, or in buildings with strong network signal interference from a large amount of mechanized equipment. Experimental results show that CLS-IL system can achieve accurate location results, and which prove that the indoor localization method has great development prospects.

The rest of this paper is arranged as follows. Introducing related works in Section 2. Section 3 introduces the phase of offline database establishment. Section 4 introduces online positioning phase of the indoor localization system based on smartphone built-in sensors and crowd-sourcing landmarks. Section 5 conducts experimental simulation and analysis of experimental results. Section 6 gives conclusions and future research work.

## II. RELATED WORKS

In this section, we have studied a mass of existing indoor positioning technologies. Among them, fingerprints (WiFi fingerprints, Bluetooth fingerprints) and mobile sensors-based technologies are the most common and popular. At present, researchers have also tried to use secondary sensors or landmarks to solve mobile sensor data, which will be affected by the environment and cause fluctuations, leading to the problem of cumulative errors. Therefore, the performance of this indoor positioning technology depends on its degree of error correction and whether these errors can be eliminated to provide the user's location accurately.

Wang *et al.* [25] proposed a Bluetooth-based trilateral measurement method by combining the Bluetooth signal transmission model and trilateral measurement and positioning method. However, this method can only estimate approximate areas of users, and cannot obtain accurate location. Kotanen *et al.* [26] used extended Kalman filter to process Bluetooth signal and designed an received signal strength indicator (RSSI) range estimation model which can obtain accurate positioning distance on the premise of receiving the signal strength accurately. However, its positioning accuracy still fluctuates in actual tests. Röbesaat *et al.* [27] proposed a position-tracking system based on BLE, in which Kalman filter was used to filter the noise in RSSI data and triangulation measurement was used for positioning. Experimental results showed that tracking effect of this system is perfect and estimate error can reach 0.75m and below, but the premise was that localization area of this experiment was limited. In addition, the dense placement of BLE modules in this experiment resulted in a significant increase in cost. Zhou *et al.* [28]

used inertial measurement unit (IMU) for indoor positioning. User's position was preliminarily estimated based on the measured inertial data. Then, the distance was measured using sound signal reflected by object near the user to correct inertial errors. User's position can be corrected based on reflected sound waves in the space if a three-dimensional space consisting of a ceiling and two walls exists. However, this method required a three-dimensional dielectric that can reflect acoustic waves, because it is difficult to detect if the acoustic produced by equipment is reflected irregularly by ordinary media.

Chattha and Naqvi [29] combined gyroscope and magnetometer sensors to propose a pedestrian dead reckoning algorithm based on smartphones. Because they all use sensors in smartphones to achieve positioning, and the data of built-in direction sensors of smartphone were prone to deviations in direction, and the PDR algorithm was prone to problems such as drift errors, some research teams have used special indoor areas (e.g., corner, etc) were set as landmarks, but the positioning accuracy in real scene was generally only room level (about 5 meters). Li et al. [30] used the location of iBeacon as a landmark and corrected path through iBeacon landmarks. However, overcorrection often occurs. Zhou et al. [31] proposed a crowdsourcing-based indoor location tracking system, which combined RSSI data of indoor structures and corresponding locations with Wi-Fi data collection results to establish landmarks. Then, user's location was calibrated by using user's movement data. However, the system was difficult to apply to all buildings because it required a corresponding indoor radio-map to obtain the information of the location area in advance. Munoz Diaz et al. [32] proposed a landmark-based heading drift compensation algorithm. Landmarks were generated by detecting stairs and corner positions in real time as user walks between buildings. When these landmarks were re-passed during the experiment, they correlated to calculate drift errors accumulated in user's walking trajectory. Then, in data processing stage, the value of drift error was converted into low drift yaw estimation by directional estimation filter, so as to realize the trajectory drift compensation. However, using inertial measurement alone to calculate drift errors in walking process cannot maintain the stability of errors for a long time. Shen et al. [33] proposed a crowdsourcing positioning system that did not require indoor flat maps. It used crowdsourcing PDR trajectories and Wi-Fi access points as landmarks to generate indoor trajectories of buildings. Under the condition that directional errors of the PDR trajectories follow zero mean Gaussian distribution, it can provide accurate walking path, but it takes a lot of time and effort to collect enough PDR trajectories. Zou et al. [34] proposed an indoor localization technology combining inertial sensor, WLAN and iBeacon. Pedestrian track estimation was performed using IMU and particle filters were used to correct sensors and fuse the data after Wi-Fi fingerprint recognition and iBeacon. However, this system not only required to deploy a large amount of infrastructure to be deployed indoors, but also required a large amount of task to upgrade router firmware.

The existing indoor positioning technologies reviewed above combine low-power Bluetooth, built-in sensors in smartphones, etc., and different models and algorithms were used to correct data errors to improve location accuracy. However, the limitation of using smart sensors for positioning lies in that they can only be used in a limited environment. When multiple complex algorithms are combined, the processing power of smartphones is lower than that of normal central processing unit (CPU), so their computing speed will be greatly reduced so that sensor reading errors cannot be corrected quickly. In addition, in these indoor positioning technologies based on landmarks, relevant literatures only consider how to add landmarks, but fail to consider large task load and system running delay caused by the redundant landmark database increasing gradually. Therefore, based on the shortcomings of above technologies, this paper proposes a system model of crowd-sourcing landmarks-assisted smartphone in indoor localization (CLS-IL). Firstly, the gyroscope sensor and magnetometer sensor are used to obtain user's position. Then, using Bluetooth beacons-based landmarks to achieve fast position correction. Finally, in the proposed landmarks correction technology, system allows users to add crowd-sourcing landmarks adaptively. It also updates the detection times of crowd-sourcing landmarks in real time and feeds the latest and most commonly used crowd-sourcing landmarks back to users to achieve dynamic optimization of the landmark database.

## III. OFFLINE PHASE

In order to solve the problem of cumulative drift errors during pedestrian dead reckoning, the limitation of visual positioning and the problem that image landmarks are easily affected by surrounding environment. A system model of crowd-sourcing landmarks-assisted smartphone in indoor localization which used low-power Bluetooth beacons as landmarks is proposed to obtain accurate pedestrian dead reckoning results in this paper. In this section, offline database establishment phase of the CLS-IL system is mainly described. Firstly, the RSSI data of Bluetooth beacon is filtered and denoised by Kalman filter to obtain stable and smooth data. Then, the beacon node is set up according to filtered data, and a database of predefined landmark is established according to defined predefined landmark rules.

### A. BEACON NODES SETTING

Offline phase includes offline beacon nodes setting and predefined landmarks setting. In preparation phase, a set of low-power Bluetooth beacons [35] are evenly arranged in interior space and represented as $\hat{N} = \{1, 2, \ldots\ldots, n\}$, which used as beacon nodes and predefined landmarks. Beacon nodes are defined as the initial starting points of indoor localization, such as the entrance of a building, an elevator or a staircase. Firstly, CLS-IL system selects the beacon node

for initial positioning in indoor environment. The properties of the $n_{th}$ beacon node $b_n$ are shown in equation (1):

$$b_n = \{x_n, y_n, L_n\}, \quad n \in \hat{N} \tag{1}$$

where $(x_n, y_n)$ is the predetermined coordinate pair of beacon node $b_n$, $RL_n$ is the RSSI list of Bluetooth beacons detected at beacon node $b_n$. The properties of $RL_n$ are illustrated in equation (2):

$$RL_n = \{(B_1, RSSI_1), (B_2, RSSI_2), \ldots\ldots, (B_n, RSSI_n)\}, n \in \hat{N} \tag{2}$$

where $B_n$ represents the $n_{th}$ low-power Bluetooth beacon, $RSSI_n$ represents the RSSI value of the $n_{th}$ low-power Bluetooth beacon. CLS-IL system stores the information of beacon node in server.

During the experiment, when users enter the building room and GPS signal disappears, user's handheld smart mobile terminal measures RSSI value of Bluetooth beacon at the current location and receives a list of beacon nodes from the server. The k-nearest neighbor (KNN) algorithm [36], [37] based on the shortest physical distance between reference points and target locations (called Euclidean distance) and works deterministically, so CLS-IL system uses KNN algorithm to search for the nearest beacon node in beacon list, which is represented in equation (3). This position is used as a starting point for indoor localization to start indoor positioning of users.

$$D_q = \sqrt{\sum_{i=1}^{n}(RSSI_{online}(i) - RSSI_q(i))^2} \tag{3}$$

where $D_q$ represents the Euclidean distance between the $q_{th}$ reference point and target, and $i$ represents the number of beacon nodes.

## B. PREDEFINED LANDMARK SETTINGS

After initial beacon nodes are set up, CLS-IL system will establish predefined landmarks based on the indoor environment. Landmarks are defined as reference points. Landmarks proposed in this paper refer to geographical locations that can be clearly distinguished from other locations in sensors data of mobile phones, which are different from those landmarks in traditional sense. In CLS-IL system, the Bluetooth beacon with a constant RSSI value obtained from repeated measurements at the special indoor location is set to a predefined landmark. As shown in Figure 2, we have tested the RSSI values of two different types of Bluetooth beacons produced by two different companies. It can be seen that two sets of RSSI values are generated with the change of sampling time due to the instability of Bluetooth system and the maximum fluctuation is about 12dBm. Therefore, in order to reduce the influence of random fluctuation of RSSI values on location accuracy, we use Kalman filter [38] to filter and denoise the collected RSSI values to obtain more accurate and smooth RSSI value distribution.
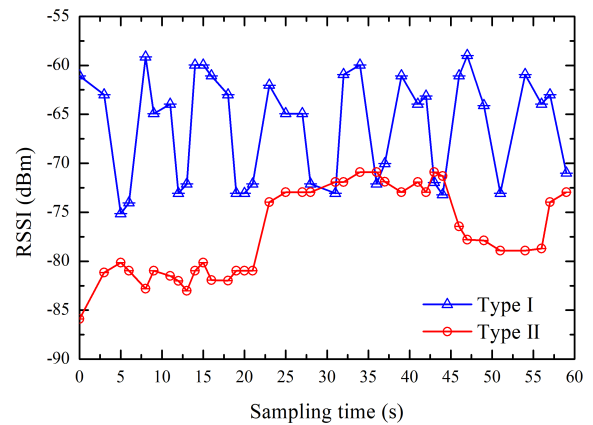


**FIGURE 2.** RSSI values of different types of Bluetooth beacons.
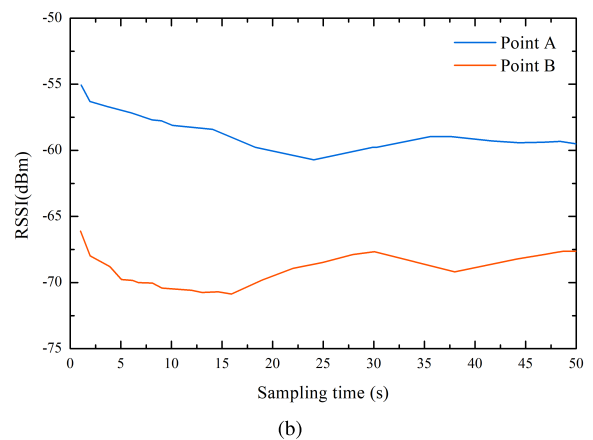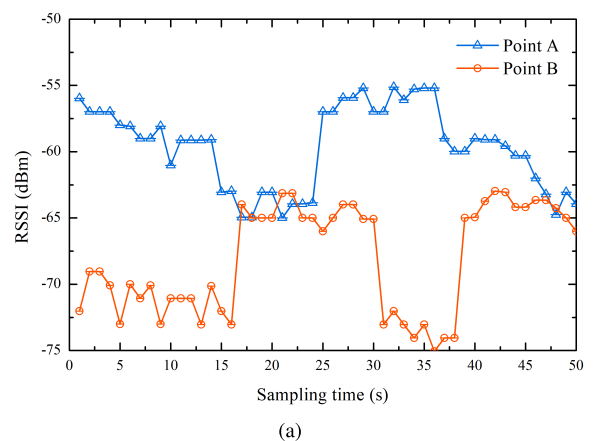


(a)



(b)

**FIGURE 3.** Comparison of RSSI values (a) original data (b) data after Kalman filtering.

We compare the original RSSI values collected at two Bluetooth beacon point A and point B in figure 7 with the RSSI values processed by Kalman filtering, the experimental results are shown in figure 3. The transmission interval of beacon frames of these two Bluetooth beacon nodes was set to 1000ms, and RSSI values were collected for 50 times continuously. It can be seen that the original RSSI data had drastic fluctuations and showed time-varying characteristics obviously. After Kalman filtering, RSSI data is more smooth, stable and reliable.
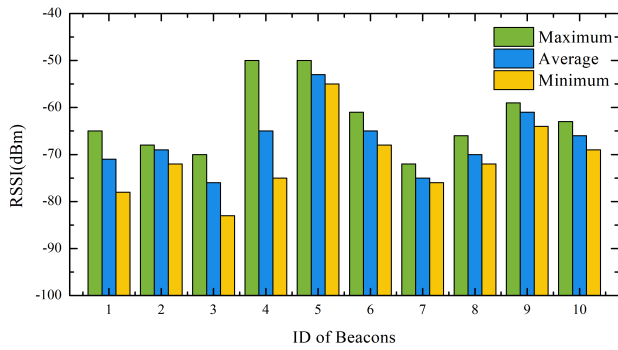
**FIGURE 4.** Example that conform the definition of predefined landmark setting.

After the above work, we give the definition of predefined landmark setting. It is required that the average of RSSI signal received by users from predefined landmarks should be greater than -70dBm during 10 measurements repeatedly, and the difference between the maximum and minimum value should not exceed 5dBm. As shown in figure 4, point2, point5, and point9 conform to above definition and they can be set as landmarks. What we want to explain here is that although beacon nodes and predefined landmarks are made of low power Bluetooth, they have different physical meanings.

When there is no network connection in indoor positioning environment and system users do not know that in advance, they will not be able to use the previously set beacon nodes or predefined landmarks, leading to location performance degradation. Therefore, the offline priority mobile application should be used to solve this problem, so that CLS-IL system users can receive the database that integrates beacon nodes and predefined landmarks in advance to guarantee that indoor localization operations can be performed in a non-network environment.

## IV. ONLINE LOCALIZATION PHASE

This section mainly describes online localization phase of CLS-IL system. Firstly, initial positioning is performed. Accelerometer is used to obtain the information of user's gait and step length, and define selection rules of sensor readings during the course estimation process according to actual environment and real-time characteristics of magnetometer and gyroscope sensors. Then, using naive Bayes classifier to detect landmarks near users, and CLS-IL system corrects user's position according to landmark database and feeds it back to current localization system. Finally, a dynamic landmark library correction algorithm is proposed to achieve adaptive optimization and accurate positioning.

### A. INITIAL POSITIONING BASED ON BUILT-IN SENSORS OF SMARTPHONE

The process of CLS-IL indoor localization system is shown in figure 5, including initial positioning phase and landmark cohrrection phase. User searches for the nearest beacon node through handheld smart terminals, so as to select and determine the starting point of location and start positioning work. Then CLS-IL system measures user's position movement by using built-in sensors of smartphone. Pedestrian navigation information is determined by three parts: gait detection, step length estimation, and heading estimation. Firstly, system measures the reading change of acceleration sensor through a step counter to detect user's movement status in real time. The real-time position of user's motion is determined by calculating the two values of moving distance and forward direction when CLS-IL system detects a change in user's motion state.

### 1) GAIT DETECTION

Peak detection is the basic method for accurate gait detection by using accelerometer. During the exercise, this method involves the vertical acceleration generated by a vertical impact when user's foot is stepping on the floor. Since vertical acceleration is affected by the tilt of smartphone, we must focus on the magnitude of vertical acceleration $a$. Gait detection needs to meet the two conditions of $|a-g| \geq a_{th}$ and $\Delta t \geq t_{th}$, where $g$ represents the gravity, $a_{th}$ represents acceleration threshold, and $t_{th}$ represents the time threshold within acceleration measurement time period $\Delta t$. Acceleration threshold $a_{th}$ is used to limit false gait detection, while time threshold $t_{th}$ is used to limit the duration of gait detection to a limited range. Acceleration and its threshold range are shown in figure 6.

### 2) STEP LENGTH ESTIMATION

User's step length varies from person to person, and the way and pace of each person's walk are different. Therefore, it has challenge to achieve a very accurate step length estimation. Step length estimation methods are divided into static method and dynamic method [39]. Static method usually assumes that the step length of user is constant in the whole positioning process, and it will only be different according to individual characteristics of different users. Therefore, this paper uses Weinberg's dynamic method [40] to estimate user's step length. According to user's actual dynamic movement. The change of each step in the process of movement is matched with different step length to provide more accurate support for navigation position estimation at the next moment. Step length $L_S$ is calculated using vertical acceleration obtained by accelerometer, as shown in equation (4):

$$L_S = k \cdot \sqrt[4]{a_{max} - a_{min}} \qquad (4)$$

where $k$ is a fixed value. In this experiment, we performed unified tests on people of different heights, and finally $k$ is set to 0.35, $a_{max}$ and $a_{min}$ are the maximum and minimum values of vertical acceleration respectively.

### 3) HEADING DIRECTION ESTIMATION

Heading direction estimation method is very important in the whole pedestrian path estimation, because heading error will seriously affect location accuracy. In this paper, heading direction estimation is obtained by fusing data from
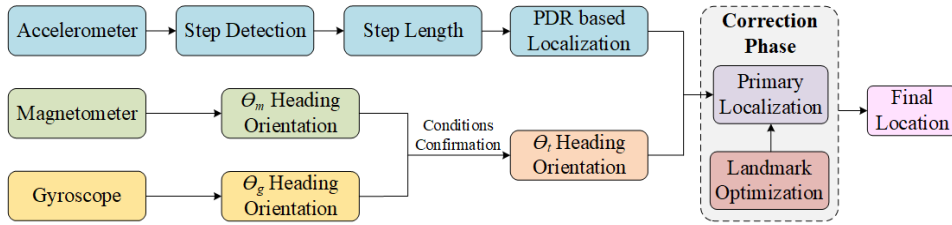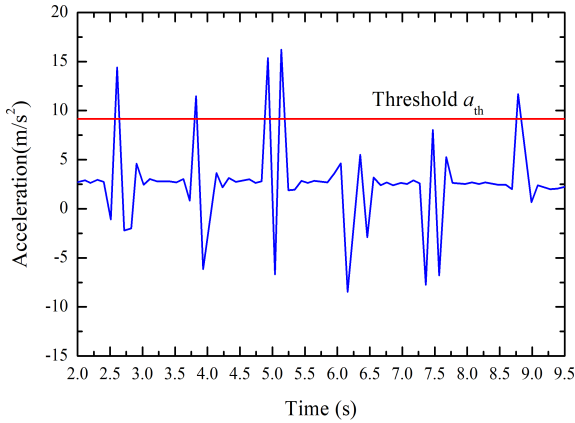
FIGURE 5. Localization process of CLS-IL system.



FIGURE 6. Acceleration and its threshold.

magnetometer sensor and gyroscope sensor. At time $t$, the value of current forward direction $\theta_t$ is calculated by calculating the value of previous forward direction $\theta_{t-1}$. The value of $\theta_t^m$ can be obtained through the fusion of reading values of accelerometer and magnetometer sensors, which can be used to measure $V^a$ and $V^m$ when CLS-IL system detects the change in the reading of magnetometer sensor, as shown in equations (5) and (6):

$$V^a = \{x^a, y^a, z^a\} \tag{5}$$
$$V^m = \{x^m, y^m, z^m\} \tag{6}$$

where $x^a$, $y^a$ and $z^a$ respectively represent the values of acceleration sensor measured on $x$, $y$, $z$ axis on the smartphone, $x^m$, $y^m$ and $z^m$ respectively represent the values of magnetometer sensor measured on $x$, $y$, $z$ axis on the smartphone. CLS-IL system converts it from an intelligent device coordinate system to orthonormal basis coordinate system. System calculates the matrix $M$, $M \in R^{3 \times 3}$ in equation (7):

$$M = \begin{bmatrix} M_{11} & M_{12} & M_{13} \\ M_{21} & M_{22} & M_{23} \\ M_{31} & M_{32} & M_{33} \end{bmatrix} \tag{7}$$

The values of accelerometer and magnetometer sensors are used to calculate the first row of matrix $M$, as shown in

equation (8):

$$\begin{cases} M_{11} = (y^m z^a - z^m y^a) \cdot \omega_1 \\ M_{12} = (z^m x^a - x^m z^a) \cdot \omega_1 \\ M_{13} = (x^m y^a - y^m x^a) \cdot \omega_1 \end{cases} \tag{8}$$

where the expression of weight coefficient $\omega_1$ is shown in equation (9):

$$\omega_1 = \frac{1}{\sqrt{(y^m z^a - z^m y^a)^2 + (z^m x^a - x^m z^a)^2 + (x^m y^a - y^m x^a)^2}} \tag{9}$$

The third line of matrix $M$ can be calculated only by using the value from accelerometer, which as shown in equation (10):

$$\begin{cases} M_{31} = x^a \cdot \omega_2 \\ M_{32} = y^a \cdot \omega_2 \\ M_{33} = z^a \cdot \omega_2 \end{cases} \tag{10}$$

where the expression of weight coefficient $\omega_2$ is shown in equation (11):

$$\omega_2 = \frac{1}{\sqrt{(x^a)^2 + (y^a)^2 + (z^a)^2}} \tag{11}$$

Finally, the second line of matrix $M$ is calculated with the first and third lines obtained previously. The calculation equation is shown in (12):

$$\begin{cases} M_{21} = M_{32} M_{13} - M_{33} M_{12} \\ M_{22} = M_{33} M_{11} - M_{32} M_{13} \\ M_{23} = M_{31} M_{12} - M_{32} M_{11} \end{cases} \tag{12}$$

CLS-IL system calculates $\theta_t^m$ according to equation (13) when the rotation matrix $M$ is calculated:

$$\theta_t^m = \arctan 2(M_{11}, M_{22}) \tag{13}$$

Next, the value of $\theta_t^g$ is calculated based on the data detected from accelerometer and gyroscope. When intelligent device tests a change in the reading of gyroscope sensor, the value $S_t^g$ of gyroscope sensor is measured, where $S_t^g$ represents the speed at which the user's heading direction changes with time $t$. Then calculate the change value $\Delta\theta^g$ of $\theta_t^g$ between adjacent moments, as shown in equation (14):

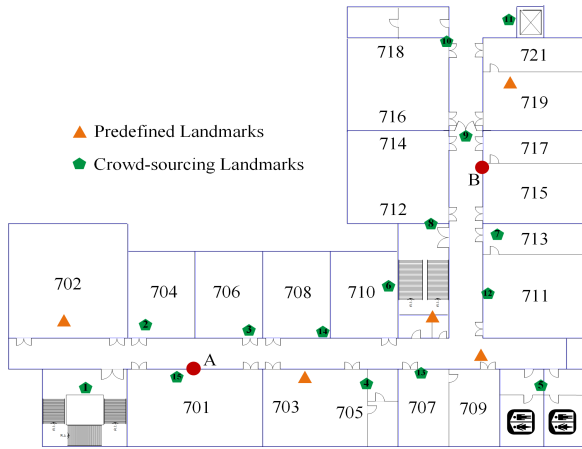$$\Delta\theta^g = \int_{t-1}^{t} S_t^g \, dt \tag{14}$$

**FIGURE 7.** Interior layout of test platform building.

At time $t$, the value of $\theta_t^g$ is calculated from the gyroscope sensor reading at time $t-1$, as shown in equation (15):

$$\theta_t^g = \theta_{t-1}^g + \Delta\theta^g \tag{15}$$

In order to evaluate the attributes of heading direction computed using gyroscope and magnetometer sensors, users performed 30 measurements using either the magnetometer sensor or the gyroscope sensor along the path shown in figure 7. It can be seen from the figure 8 that the value of magnetometer is almost constant at the same position, but the value of gyroscope sensor fluctuates. Therefore, we believe that alternating calculations using gyroscope sensor and magnetometer sensor can obtain a more accurate heading direction of user. According to the value proportion of these two values in experimental results, CLS-IL system calculates heading direction according to the values of $\theta_t^g$ and $\theta_t^m$ using the following algorithm which as shown in equation (16):

$$\theta_t = \begin{cases} \theta_t^m, & (\theta_{t-1} + \Delta\theta^g > \theta_t^m, \Delta\theta^g > lim^\theta) \\ \theta_t^g, & (\theta_{t-1} + \Delta\theta^g \le \theta_t^m, \Delta\theta^g > lim^\theta) \\ \theta_{t-1}, & (\Delta\theta^g \le lim^\theta) \end{cases} \tag{16}$$

where $lim^\theta$ is the ultimate value of $\Delta\theta^g$. According to this value, the variation degree of previous readings of gyroscope sensor can be observed. CLS-IL system calculates the heading on the basis of three conditions in equation (16). In the first case, $\Delta\theta^g$ is greater than $lim^\theta$, and reading value $\theta_t^m$ of magnetometer is less than the sum of previous forward direction $\theta_{t-1}$ and $\Delta\theta^g$. It indicates that CLS-IL system can accurately detect the rotation angle of users based on magnetometer sensors, so the value of $\theta_t^m$ is used to calculate heading direction in this case. In the second case, rotation angle can be detected if $\Delta\theta^g$ is greater than $lim^\theta$, while the sum of $\theta_{t-1}$ and $\Delta\theta^g$ is smaller than $\theta_t^m$. But the estimations are not accurate enough, because magnetometers are greatly influenced by ambient environment, so the value of $\theta_t^g$ is used to calculate heading direction in this case. In the last case,
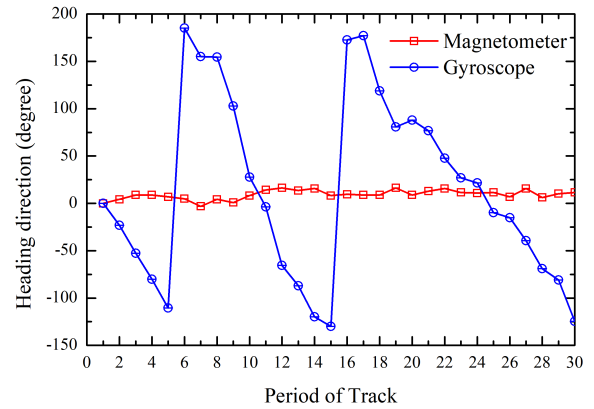


(a)
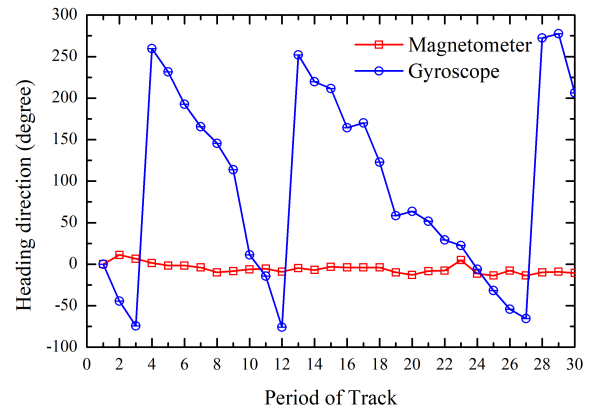


(b)

**FIGURE 8.** Heading direction at (a) point A and (b) point B in Figure 7.

if $\Delta\theta^g$ is less than $lim^\theta$, that means there is no significant rotation in user's direction of motion. Therefore, the $\theta_{t-1}$ value of the previous time is used to calculate heading direction of the next time.

The real-time coordinates of user in the room are obtained based on the fusion of previously calculated user's moving distance and moving heading. Calculate user's current coordinate $(x_t, y_t)$ according to equation (17):

$$\begin{cases} x_t = x_{t-1} + \Delta x \\ y_t = y_{t-1} + \Delta y \end{cases} \tag{17}$$

where $\Delta x$ and $\Delta y$ are calculated by using the sine and cosine of $\theta_t$, as shown in equation (18):

$$\begin{cases} \Delta x = d_t \cos(\theta_t) \\ \Delta y = d_t \sin(\theta_t) \end{cases} \tag{18}$$

## B. LANDMARK DETECTION
During the online localization phase based on the built-in sensors of smartphones, CLS-IL system will perform gait detection, step length estimation, heading direction estimation and correction for users. However, the measured position of user is not accurate enough at this time, because the position is calculated by using the previous position. Assuming that there

are no other reference points in the positioning process, then the measured position may be wrong and may be accumulated by errors which leading to excessive positioning errors. Therefore, CLS-IL system will use landmarks to correct the resulting errors due to drift.

A proximity radius is defined for each landmark during the detection phase of landmark proximity. The problem of landmark detection can be regarded as a binary classification problem. Here, we use Naive Bayes classifier [41] to detect landmarks near users. For each landmark, there are only two possible outcomes. Either user is close to landmark (that is, within the proximity radius of landmark) or not near landmark (that is, the user is outside the proximity radius of landmark). The probabilistic model for Naive Bayes classifier was trained based on RSSI data collected at different distances. During the marking process, all RSSI measurements collected within the radius are marked as 1, and the rest marked as 0. The conditional probability model of each landmark can be calculated by using equation (19):

$$p(C_j^k | \varphi_j^1, \varphi_j^2, \ldots\ldots, \varphi_j^n) \propto p(C_j^k, \varphi_j^1, \varphi_j^2, \ldots\ldots, \varphi_j^n) \quad (19)$$

where $\varphi_j^i$ represents the $i_{th}$ RSSI measurement value of landmark $j$, $C_j^k$ denotes the $k$ classification of landmark $j$. It is defined as the user is close to landmark when $k = 1$, otherwise, user is not within the coverage of landmarks when $k = 0$.

The joint model can be expressed as equation (20):

$$p(C_j^k, \varphi_j^1, \varphi_j^2, \ldots\ldots, \varphi_j^n) = p(C_j^k)p(\varphi_j^1|C_j^k)p(\varphi_j^2|C_j^k)\ldots$$
$$= p(C_j^k)\prod_{i=1}^{n} p(\varphi_j^i|C_j^k) \quad (20)$$

Finally, make a decision on landmark proximity detection by using equation (21):

$$\phi_j = \underset{k \in \{0,1\}}{\arg \max} \, p(C_j^k)\prod_{i=1}^{n} p(\varphi_j^i|C_j^k) \quad (21)$$

where $n$ represents the measured value of RSSI collected by the Bluetooth beacon which corresponding to landmark $j$, $\phi_j$ denotes the estimation classification of landmark $j$.

### C. ADAPTIVE OPTIMIZATION OF LANDMARK DATABASE
Algorithm 1 represents the pseudocode of adaptive optimization algorithm for landmark database (AOLMs). Whenever CLS-IL system starts to calculate the location of user, it will check the measured value $D_V$ and the distance between currently calculated position of user and all landmarks. $D_V$ has the property of Boolean, therefore, it is used to check whether the landmark was previously detected. If $D_V$ is true, it means that system has previously entered the landmark into database, which can effectively prevent system from locking to the same landmark continuously. The physical distance between landmark and user's location is calculated by equation (22):

$$d = \sqrt{(x^{lm} - x_t)^2 + (y^{lm} - y_t)^2} \quad (22)$$

---

**Algorithm 1** Pseudocode for AOLMs

1: For all Detected distance values ($D_V$) in the CLS-IL
2: **if** ($D_V == false$ && $d < lim^d$) **then**
3:     Compare RSSI lists of beacons ($RL_b$) and predefined landmarks ($RL_{lm}$)
4:     **if** ($RL_b$ is similar to $RL_{lm}$) **then**
5:         *set_AllLandmarks_$D_V$(false)*
6:         $(x_t, y_t) = (x_{lm}, y_{lm})$
7:     **end if**
8: **end if**
9: **if** ($D_V == true$ && $lm \in crowd\_lm$) **then**
10:     **for** $num^{lm} = 1 : n$ **do**
11:         $num^{lm} \leftarrow num^{lm} + +$
12:     **end for**
13: **end if**
14: **if** ($RL_b$ satisfied *condition_lm*) **then**
15:     *new_lm* $= (x_t, y_t, RL_b, false, 0)$
16:     add *new_lm* to *crowd_lm*
17: **end if**
18: **for** $n = 1 : crowd\_lm$ **do**
19:     $num^{lm} \leftarrow 0$
20: **end for**

---

$lim^d$ is the limit value of $d$, which is used by CLS-IL system to judge whether user's location is close enough to landmark. If $D_V$ is false and the distance is less than $lim^d$, then the RSSI data list for Bluetooth beacons at the current location is compared to the RSSI data list for predefined landmarks that have been preset. If the two lists are similar, user's location calculated at this time will be forced to move to the nearest landmark position by the system. In actual positioning process, if RSSI value of Bluetooth beacon detected by user meets the requirements of RSSI value of predefined landmark we set, then CLS-IL system allows user to add it to landmark database as trusted crowd-sourcing landmarks for subsequent use. There will have jumping points during the experiment. The accuracy of localization will not be improved when the number of landmarks is exceeded, and even too many Bluetooth devices can cause signal interference. Therefore, overcrowded landmarks cannot be believable completely, which are only worth using for reference. So CLS-IL system server will manage them individually, managing the number of checks for each landmark. Whenever new landmarks will be found by users, they will be sent to system server and will be added to crowd-sourcing landmarks list temporarily. Then, these data will send to the system user at the next update. And it will feed back to system server whenever user detects a landmark, and then the server accumulates the number of times this landmark is detected. Then the number of detections for this landmark will be accumulated by server. The server will send users a list of the most frequently detected landmarks periodically. In addition, server will periodically reset landmark database and reset the detection number of crowd-sourcing

landmarks to zero so as to clear unused landmarks in the database.

## V. EXPERIMENTAL AND SIMULATION ANALYSIS

### A. EXPERIMENTAL DEPLOYMENT

This section evaluates the performance of CLS-IL system. Numerous experiments are performed in the environment of the seventh floor of physical experiment building shown in figure 7. The area of experimental scene is $26 \times 14.6 = 379.6$ square meters. Users fixed their smartphones to chests to minimize the probability of sensor errors in each experiment. Orange triangles represent predefined landmarks which are normally used by default for all experiments. Green pentagons are crowd-sourcing landmarks added after adaptive optimization. The numbers above represent the order in which they are added. Here we store the coordinates of experimenters at 8 points in experiment path. It took an average of one minute for users to complete a journey along this path. The smart device used in the experiment is Huawei Honor 10 which includes acceleration sensor, magnetometer sensor and gyroscope sensor; Bluetooth Low Energy Beacon used the Mini Beacon with 3V CR2477 battery; PostgreSQL was used as the server of CLS-IL system to manage landmark database.

We contrast CLS-IL system with the following five methods so as to evaluate the practicability and scalability of CLS-IL system more accurately.

1) SILm: Indoor localization technology only using magnetometer sensor built into smartphone.
2) SILg: Indoor localization technology only using gyroscope sensor built into smartphone.
3) SILmg: Indoor localization technology using a combination of magnetometer sensor and gyroscope sensor built into smartphone.
4) PLS-IL: Indoor localization technology based on predefined landmarks assisted smartphone built-in magnetometer sensor and gyroscope sensor without adaptive optimization of landmark database.
5) CLS-ILmap: This technology based on the CLS-IL system proposed in this article which adds an indoor map for reference to verify the scalability of CLS-IL system. CLS-ILmap achieves accurate indoor localization by excluding unreachable areas while knowing indoor map. The core idea of this extension is that the system will determine that user's forward direction is wrong at this time when user's estimated position is an unreachable area, so the heading direction will be changed by $1°$, and the changed forward direction and forward direction will be used to calculate user's new location. At this moment, system will ready to change direction to left and right at the same time to find the faster direction of distance to accessible area as a new heading. Then this heading and location will be used to support subsequent localization.
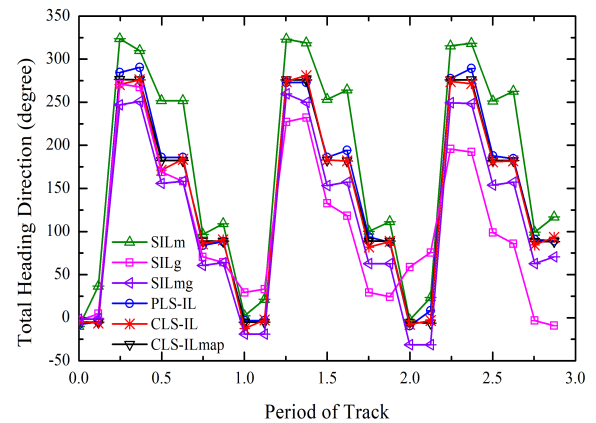


**FIGURE 9.** Comparison of heading direction estimation errors of different methods.

### B. EXPERIMENTAL RESULTS AND ANALYSIS

#### 1) ESTIMATION ERROR OF HEADING DIRECTION

Figure 9 shows the experimental results of heading direction estimation for six technologies of SILm, SILg, SILmg, PLS-IL, CLS-IL and CLS-ILmap. Horizontal axis represents the number of times that user has walked on experimental path, vertical axis indicates forward direction. Experimental results show that the heading direction estimation of SILm is quite different from the reference direction of actual path. However, the magnitude of this difference is consistent with the increase in the number of experimental paths. This is because it has been found in the experimental results of figure 9 that the data from magnetometer is nearly consistent at the same position. Heading direction estimation of SILg is similar to the reference direction at the beginning of experimental path, but heading errors will gradually increase with the increase of experiment number. The reason of that is the forward direction of SILg is calculated based on the previous forward direction, which causes a problem of error accumulation. The performance of SILmg is better than that of SILm and SILg, because SILmg technology mixes magnetometer sensors and gyroscope sensors to expand the scope of course, thus improving the accuracy of heading direction estimation. The performance of PLS-IL is better than that of SILmg. CLS-IL has better property than PLS-IL. However, the accuracy of CLS-ILmap is slightly higher than CLS-IL in the case of knowing indoor maps in advance, but the complexity of this technology is so high that it is difficult to cover all buildings for indoor positioning. Finally, the maximum, minimum, and average heading direction errors of six technologies are listed in table 1.

Figure 10 shows the experimental results of cumulative distribution function of heading direction estimation errors for SILm, SILg, SILmg, PLS-IL, CLS-IL and CLS-ILmap technologies. In 80% cases, the heading direction error of SILm is less than $50°$, the error of SILmg is less than $20°$, the errors of PLS-IL and CLS-IL are both less than $10°$, and the heading estimation result of SILg is much worse than

**TABLE 1.** Maximum, minimum, and average heading errors for six technologies.

| Heading | SILm | SILg | SILmg | PLS-IL | CLS-IL | CLS-ILmap |
|---------|------|------|-------|--------|--------|-----------|
| Maximum | 82° | 336° | 34° | 27° | 22° | 18° |
| Minimum | 1° | 3° | 1° | 1° | 0° | 0° |
| Average | 38.466° | 127.832° | 11.092° | 5.569° | 5.152° | 4.337° |

**TABLE 2.** Maximum, minimum, and average diatance errors for six technologies.

| Distance (m) | SILm | SILg | SILmg | PLS-IL | CLS-IL | CLS-ILmap |
|--------------|------|------|-------|--------|--------|-----------|
| Maximum | 450.268 | 127.854 | 58.083 | 37.862 | 33.189 | 10.224 |
| Minimum | 45.517 | 2.286 | 3.890 | 0.646 | 0.298 | 0.121 |
| Average | 224.102 | 38.226 | 29.118 | 13.211 | 10.858 | 3.738 |



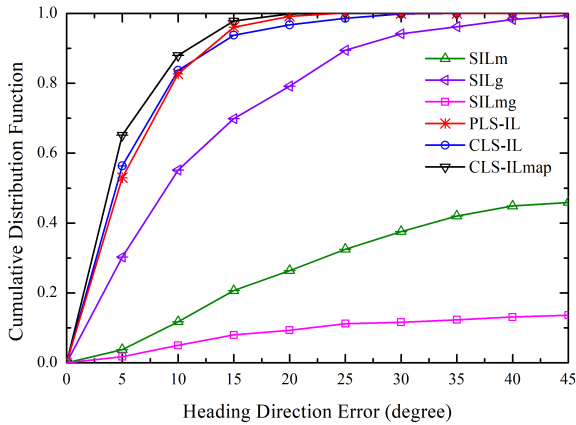**FIGURE 10.** Cumulative distribution function of heading errors.



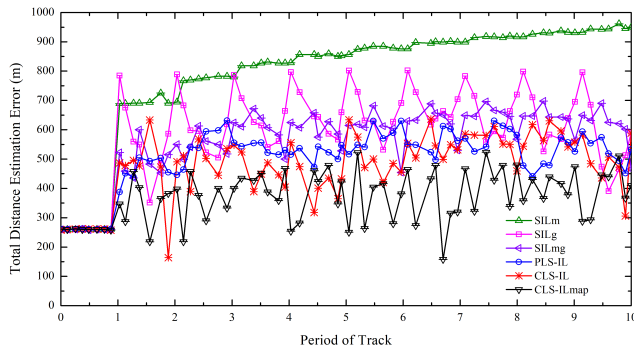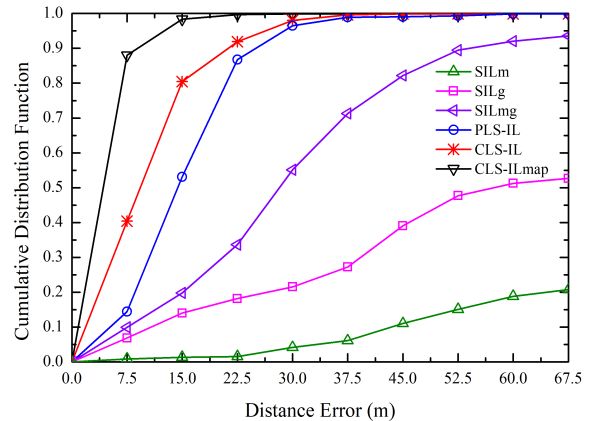**FIGURE 12.** Cumulative distribution function of distance errors.



**FIGURE 11.** Comparison of distance estimation errors between different technologies.

other technologies. It can be seen that SILmg is superior to SILm and SILg, PLS-IL and CLS-IL have greater advantages than SILmg, while the accuracy of CLS-IL was similar to that of PLS-IL in terms of heading direction estimation. Finally, CLS-ILmap demonstrates the best performance by excluding unreachable areas. It can be proved that the indirect correction of landmarks to heading estimation are effective.

### 2) ESTIMATION ERROR OF DISTANCE

Figure 11 shows the experimental results of distance estimation errors for SILm, SILg, SILmg, PLS-IL, CLS-IL, and CLS-ILmap technologies under references of actual path. The maximum, minimum and average distance errors of six technologies are listed in table 2. It can be found that the distance errors obtained by different technologies are different. The distance errors obtained by the six methods are almost zero during the first path, which shows that all technologies

maintained good performance in early stage of experiment. However, the distance errors all changed and showed an overall upward trend with increase of the number of experiments. Experimental results show that the distance error obtained by using magnetometer sensor or gyroscope sensor alone is the largest and location accuracy is the lowest. The localization error has been significantly reduced after the combination of magnetometer and gyroscope. The location error has been significantly reduced, and location accuracy has also been significantly increased after the introduction of landmarks, and CLS-IL technology based on crowd-sourcing landmarks performed better than PLS-IL which only used predefined landmarks. Finally, CLS-ILmap technology achieved the minimum location error by excluding unreachable regions, but the complexity of this technology is higher than other technologies.

Figure 12 shows the experimental results of cumulative distribution function of distance estimation errors for SILm, SILg, SILmg, PLS-IL, CLS-IL and CLS-ILmap technologies. Performed real-time localization on user's position at 8 points that have been stored in the path.

Experimental results show that in about 80% cases, the cumulative distance estimation error is less than 65 meters for SILg and less than 43 meters for SILmg. For PLS-IL and CLS-IL, the cumulative distance estimation errors are less than 22 meters and 15 meters respectively. The cumulative distance error of SILm is the largest and localization effect is the worst. It can be seen that the performance of SILmg is better than that of SILm and SILg, but the error will be cumulatively increased if an error occurs during positioning process, because there is no reference node, which will gradually reduce positioning performance. In contrast,
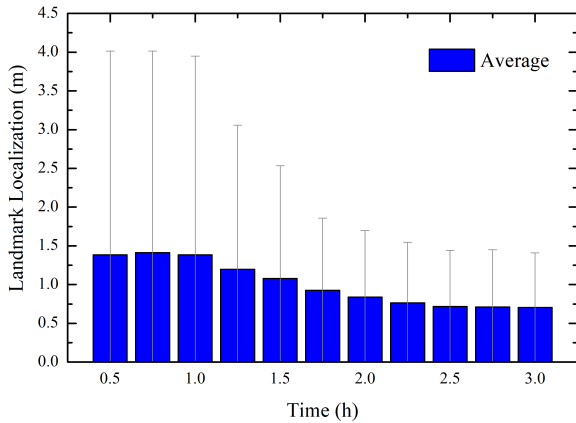
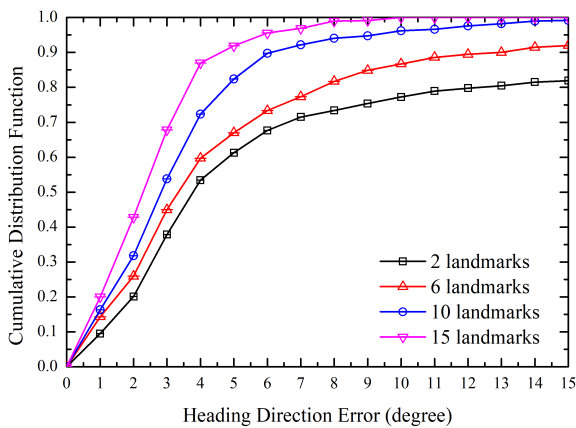**FIGURE 13.** The accuracy of landmarks localization varies with time.



**FIGURE 14.** Cumulative heading errors distribution under different crowd-sourcing landmarks.



**FIGURE 15.** Cumulative distance errors distribution under different crowd-sourcing landmarks.

PLS-IL can effectively reduce distance errors due to the introduction of predefined landmarks. However, CLS-IL based on crowd-sourcing landmarks has better positioning performance than PLS-IL on the basis of dynamic optimization of landmark database.

### 3) CROWD-SOURCING LANDMARKS

Figure 13 shows the variation in average location accuracy of calculated landmarks over time. The number of landmarks obtained in the environment will increase over time as more users participate in experiment. In fact, the experimental data is limited in path diversity due to the limitation of moving area. In practical applications, the increase of path diversity may improve location accuracy.

Figure 14 shows the experimental results of cumulative error distribution of 8 times heading estimation obtained under different numbers of crowd-sourcing landmarks. Here we set up all predefined landmarks to be used in all experiments, and each user can use crowd-sourcing landmarks detected by previous users and added to landmark database. The results show that heading error gradually decreased with the increase of landmarks in the group. However, there will be no significant improvement in heading accuracy
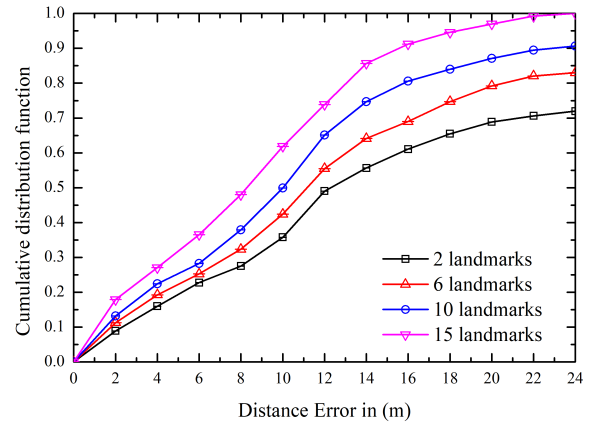
and calculations will increase considerably if landmarks continue to increase. Therefore, the performance of heading estimation has basically reached saturation when using 15 crowd-sourcing landmarks with a median accuracy of about 2.4°. In fact, due to the limitation of moving area, the data in experiment will also be limited by path diversity, which will affect location accuracy.

Figure 15 shows the experimental results of cumulative error distribution of 8 times distance estimation obtained under different numbers of crowd-sourcing landmarks. Here we also set up all predefined landmarks to be used in all experiments, and each user can use crowd-sourcing landmarks detected by previous users and added to landmark database. The results show that the distance estimation error has gradually decreased as landmarks increase. When using 15 crowd-sourcing landmarks, the CDF of location error has exceeded 0.85 with an error within 14 meters, and the CDF has exceeded 0.9 with an error within 16 meters, average median location error is about 1.04m. And the mean median error is 1.25 meters when just 10 landmarks are used. It can be seen that location accuracy gradually increases while the crowd-sourcing landmarks increasing. However, location accuracy will not change significantly with increase of landmarks when the number of landmarks has reached saturation. Instead, it will result in a significant increase in workload and complexity.

### 4) COMPARISON WITH OTHER SYSTEMS

CLS-IL system was compared with two other typical systems: SoundMark peer-assisted dead reckoning system [42] and magnetic fingerprint recognition system [43]. The results in Figure 16 show that the median location error of CLS-IL is about 1.05m, which is the smallest of three systems, about 1.25m in magnetic fingerprint system, and approximately 1.34m in SoundMark peer-assisted dead reckoning system. In addition, the CDF of location error of CLS-IL system exceeded 80% within 1.56m and 90% within 1.99m, which was obviously better than other systems.
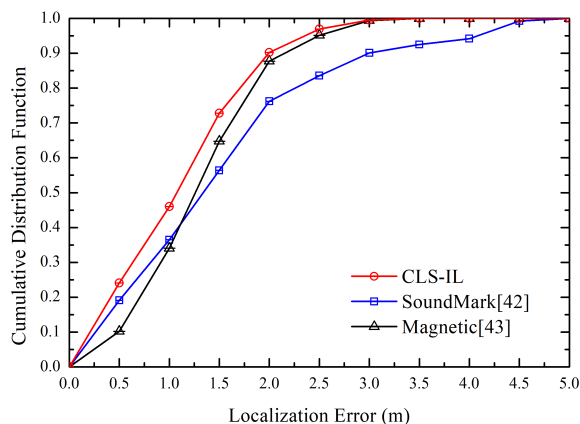
**FIGURE 16.** Comparison of CLS-IL system with two other typical systems.

## VI. CONCLUSION

A high-precision indoor localization technology based on landmark-assisted correction of built-in sensors in smartphones was proposed so as to avoid the problem of cumulative errors in traditional pedestrian dead reckoning. Landmarks were used to compensate for drift errors during pedestrian dead reckoning. Firstly, preliminary localization was performed and used accelerometer to estimate the user's gait and step length. The selection criteria of sensor reading value in heading estimation was defined by analyzing the real-time characteristics of magnetometer and gyroscope sensors through numerous experiments. Then, landmarks were introduced on the basis of preliminary localization to compensate for dead reckoning errors. Naive Bayesian classifier was used to detect landmarks near users and an adaptive optimization algorithm of landmark database was proposed, which provided a detailed localization process and verified the feasibility and scalability of landmark idea. Finally, simulation experiments and results analysis were performed from multiple aspects. Experimental results showed that location error can be rapidly converged after introducing landmarks, and the final median location error reached 1.05m, which greatly improved the indoor location accuracy. Compared with two classical positioning algorithms, CLS-IL also had obvious advantages in location accuracy. And the location accuracy will be further improved if system obtains the indoor map in advance, however, the workload is so large that it is difficult to popularize it in all buildings. Therefore, the future research direction is to integrate the construction of indoor radio maps into CLS-IL system to further improve location accuracy and scalability of the system.

## REFERENCES

[1] T. H. N. Vu, K. H. Ryu, and N. Park, "A method for predicting future location of mobile user for location-based services system," *Comput. Ind. Eng.*, vol. 57, no. 1, pp. 91–105, Aug. 2009.

[2] Z. Guan, B. Zhang, Y. Zhang, S. Zhang, and F. Wang, "Delaunay triangulation based localization scheme," in *Proc. 29th Chin. Control Decis. Conf. (CCDC)*, Chongqing, China, May 2017, pp. 2627–2631.

[3] P. Davidson and R. Piché, "A survey of selected indoor positioning methods for smartphones," *IEEE Commun. Surveys Tuts.*, vol. 19, no. 2, pp. 1347–1370, 2nd Quart., 2017.

[4] Z. Zhou, M. Kavehrad, and D. Peng, "Indoor positioning algorithm using light-emitting diode visible light communications," *Opt. Eng.*, vol. 51, no. 8, Aug. 2012, Art. no. 085009.

[5] S. Gezici, Z. Tian, G. B. Giannakis, H. Kobayashi, A. F. Molisch, H. V. Poor, and Z. Sahinoglu, "Localization via ultra-wideband radios: A look at positioning aspects for future sensor networks," *IEEE Signal Process. Mag.*, vol. 22, no. 4, pp. 70–84, Jul. 2005.

[6] Y. Wang, Q. Ye, J. Cheng, and L. Wang, "RSSI-based Bluetooth indoor localization," in *Proc. 11th Int. Conf. Mobile Ad-Hoc Sensor Netw. (MSN)*, Shenzhen, China, Dec. 2015, pp. 165–171.

[7] T. Willemsen, F. Keller, and H. Sternberg, "Concept for building a MEMS based indoor localization system," in *Proc. Int. Conf. Indoor Positioning Indoor Navigat. (IPIN)*, Busan, South Korea, Oct. 2014, pp. 1–10.

[8] B. Yang, Y. Lei, and B. Yan, "Distributed multi-human location algorithm using naive Bayes classifier for a binary pyroelectric infrared sensor tracking system," *IEEE Sensors J.*, vol. 16, no. 1, pp. 216–223, Jan. 2016.

[9] J. Kim and H. Jun, "Vision-based location positioning using augmented reality for indoor navigation," *IEEE Trans. Consum. Electron.*, vol. 54, no. 3, pp. 954–962, Aug. 2008.

[10] V. Pasku, A. D. Angelis, M. Dionigi, G. De Angelis, A. Moschitta, and P. Carbone, "A positioning system based on low-frequency magnetic fields," *IEEE Trans. Ind. Electron.*, vol. 63, no. 4, pp. 2457–2468, Apr. 2016.

[11] H.-Y. Kung, S. Chaisit, and N. T. M. Phuong, "Optimization of an RFID location identification scheme based on the neural network," *Int. J. Commun. Syst.*, vol. 28, no. 4, pp. 625–644, Mar. 2015.

[12] Y. T. Chan, W. Y. Tsui, H. C. So, and P.-C. Ching, "Time-of-arrival based localization under NLOS conditions," *IEEE Trans. Veh. Technol.*, vol. 55, no. 1, pp. 17–24, Jan. 2006.

[13] M. Scherhaufl, M. Pichler, E. Schimback, D. J. Müller, A. Ziroff, and A. Stelzer, "Indoor localization of passive UHF RFID tags based on phase-of-arrival evaluation," *IEEE Trans. Microw. Theory Techn.*, vol. 61, no. 12, pp. 4724–4729, Dec. 2013.

[14] L. W. Fullerton, J. L. Richards, and I. A. Cowie, "System and method for position determination by impulse radio using round trip time-of-flight," U.S. Patent 6 611 234, Aug. 26, 2003.

[15] N. Swangmuang and P. Krishnamurthy, "Location fingerprint analyses toward efficient indoor positioning," in *Proc. 6th Annu. IEEE Int. Conf. Pervas. Comput. Commun. (PerCom)*, Mar. 2008, pp. 100–109.

[16] J. Huang, D. Millman, M. Quigley, D. Stavens, S. Thrun, and A. Aggarwal, "Efficient, generalized indoor WiFi GraphSLAM," in *Proc. ICRA*, May 2011, pp. 1038–1043.

[17] B. D. Ferris, D. Fox, and N. D. Lawrence, "WiFi-SLAM using Gaussian process latent variable models," in *Proc. IJCAI*, Jan. 2007, pp. 2480–2485.

[18] J. Yang and Y. Chen, "Indoor localization using improved RSS-based lateration methods," in *Proc. IEEE Global Telecommun. Conf. (GLOBECOM)*, Nov. 2009, pp. 1–6.

[19] M. Azizyan, I. Constandache, and R. R. Choudhury, "SurroundSense: Mobile phone localization via ambience fingerprinting," in *Proc. MobiCom*, 2009, pp. 261–272.

[20] W.-J. Yi, W. Jia, and J. Saniie, "Mobile sensor data collector using Android smartphone," in *Proc. IEEE 55th Int. Midwest Symp. Circuits Syst. (MWSCAS)*, Boise, ID, USA, Aug. 2012, pp. 956–959.

[21] A. Mylonas, V. Meletiadis, L. Mitrou, and D. Gritzalis, "Smartphone sensor data as digital evidence," *Comput. Secur.*, vol. 38, pp. 51–75, Oct. 2013.

[22] L. Bruno and P. Robertson, "WiSLAM: Improving FootSLAM with WiFi," in *Proc. Int. Conf. Indoor Positioning Indoor Navigat.*, Sep. 2011, pp. 1–10.

[23] X. Liu, Y. Zhan, and J. Cen, "An energy-efficient crowd-sourcing-based indoor automatic localization system," *IEEE Sensors J.*, vol. 18, no. 14, pp. 6009–6022, Jul. 2018.

[24] B. Zhou, Q. Li, Q. Mao, W. Tu, and X. Zhang, "Activity sequence-based indoor pedestrian localization using smartphones," *IEEE Trans. Human-Mach. Syst.*, vol. 45, no. 5, pp. 562–574, Oct. 2015.

[25] Y. Wang, X. Yang, Y. Zhao, Y. Liu, and L. Cuthbert, "Bluetooth positioning using RSSI and triangulation methods," in *Proc. IEEE 10th Consum. Commun. Netw. Conf. (CCNC)*, Las Vegas, NV, USA, Jan. 2013, pp. 837–842.

[26] A. Kotanen, M. Hannikainen, H. Leppakoski, and T. D. Hamalainen, "Experiments on local positioning with bluetooth," in *Proc. Int. Conf. Inf. Technol., Coding Comput. (ITCC)*, Las Vegas, NV, USA, Apr. 2003, pp. 297–303.

[27] J. Röbesaat, P. Zhang, M. Abdelaal, and O. Theel, "An improved BLE indoor localization with Kalman-based fusion: An experimental study," *Sensors*, vol. 17, no. 5, p. 951, 2017.

[28] B. Zhou, M. Elbadry, R. Gao, and F. Ye, "BatTracker: High precision infrastructure-free mobile device tracking in indoor environments," in *Proc. 15th ACM Conf. Embedded Netw. Sensor Syst. (SenSys)*, Delft, The Netherlands, Nov. 2017, p. 13.

[29] M. A. Chattha and I. H. Naqvi, "PiLoT: A precise IMU based localization technique for smart phone users," in *Proc. IEEE 84th Veh. Technol. Conf. (VTC-Fall)*, Sep. 2016, pp. 1–5.

[30] Y. Li, Y. Guo, and H. Luo, "Accurate indoor localization based on the inertial navigation and the iBeacon," in *Proc. IEEE Int. Conf. Consum. Electron.-Taiwan (ICCE-TW)*, May 2016, pp. 1–2.

[31] B. Zhou, Q. Li, Q. Mao, and W. Tu, "A robust crowdsourcing-based indoor localization system," *Sensors*, vol. 17, no. 4, p. 864, 2017.

[32] E. Munoz Diaz, M. Caamano, and F. Sánchez, "Landmark-based drift compensation algorithm for inertial pedestrian navigation," *Sensors*, vol. 17, no. 7, p. 1555, 2017.

[33] G. Shen, Z. Chen, Y. Zhang, T. Moscibroda, and P. Zhang, "Walkie–Markie: Indoor pathway mapping made easy," in *Proc. USENIX Assoc. 10th USENIX Symp. Netw. Syst. Design Implement. (NSDI)*, 2013, pp. 85–98.

[34] H. Zou, Z. Chen, H. Jiang, L. Xie, and C. Spanos, "Accurate indoor localization and tracking using mobile phone inertial sensors, WiFi and iBeacon," in *Proc. IEEE Int. Symp. Inertial Sensors Syst. (INERTIAL)*, Kauai, HI, USA, Mar. 2017, pp. 1–4.

[35] W. S. Jeon and D. G. Jeong, "Enhanced channel access for connection state of Bluetooth low energy networks," *IEEE Trans. Veh. Technol.*, vol. 66, no. 9, pp. 8469–8481, Sep. 2017.

[36] B. Shin, T. Lee, and J. H. Lee "Enhanced weighted K-nearest neighbor algorithm for indoor Wi-Fi positioning systems," in *Proc. 8th Int. Conf. Comput. Technol. Inf. Manage. (NCM ICNIT)*, Seoul, South Korea, vol. 2, Apr. 2012, pp. 574–577.

[37] J. Machaj, P. Brida, and R. Piche, "Rank based fingerprinting algorithm for indoor positioning," in *Proc. Int. Conf. Indoor Positioning Indoor Navigat.*, Guimaraes, Portugal, Sep. 2011, pp. 1–6.

[38] Z. S. Houssaini, I. Zaimi, M. Drissi, M. Oumsis, and S. E. A. Ouatik, "Trade-off between accuracy, cost, and QoS using a beacon-on-demand strategy and Kalman filtering over a VANET," *Digit. Commun. Netw.*, vol. 4, no. 1, pp. 13–26, Feb. 2018.

[39] N.-H. Ho, P. Truong, and G.-M. Jeong, "Step-detection and adaptive step-length estimation for pedestrian dead-reckoning at various walking speeds using a smartphone," *Sensors*, vol. 16, no. 9, p. 1423, Sep. 2016.

[40] A. R. Jimenez, F. Seco, C. Prieto, and J. Guevara, "A comparison of pedestrian dead-reckoning algorithms using a low-cost MEMS IMU," in *Proc. IEEE Int. Symp. Intell. Signal Process.*, Aug. 2009, pp. 37–42.

[41] X. Wu, V. Kumar, J. R. Quinlan, J. Ghosh, Q. Yang, H. Motoda, G. J. McLachlan, A. Ng, B. Liu, P. S. Yu, Z.-H. Zhou, M. Steinbach, D. J. Hand, and D. Steinberg, "Top 10 algorithms in data mining," *Knowl. Inf. Syst.*, vol. 14, no. 1, pp. 1–37, 2008.

[42] H. Chen, F. Li, and Y. Wang, "SoundMark: Accurate indoor localization via peer-assisted dead reckoning," *IEEE Internet Things J.*, vol. 5, no. 6, pp. 4803–4815, Dec. 2018.

[43] H. Xie, T. Gu, X. Tao, H. Ye, and J. Lv, "MaLoc: A practical magnetic fingerprinting approach to indoor localization using smartphones," in *Proc. ACM Int. Joint Conf. Pervasive Ubiquitous Comput. UbiComp Adjunct*, Seattle, WA, USA, Sep. 2014, pp. 243–253.

**DANYANG QIN** (Member, IEEE) received the B.Sc. degree in communication engineering and the M.Sc. and Ph.D. degrees in information and communication system from the Harbin Institute of Technology in 2006, 2008, and 2011, respectively. She is currently a Professor with the School of Electronics Engineering, Heilongjiang University. Her current researches include wireless sensor networks, wireless multi-hop routing and ubiquitous sensing, positioning technology, and location-based services.

**RUOLIN GUO** received the bachelor's degree in communication engineering from Heilongjiang University, in 2018. She is currently a Postgraduate Fellow with the School of Electronics Engineering, Heilongjiang University. She has been a member of the Advance Ubiquitous Networking Communication Team. Her current research interests include the key technologies include wireless sensor networks, positioning technology, and location-based services.

**MIN ZHAO** received the bachelor's degree in communication engineering from Heilongjiang University, in 2018. She is currently a Postgraduate Fellow with the School of Electronics Engineering, Heilongjiang University. She has been a member of the Advance Ubiquitous Networking Communication Team. Her current research interests include the key technologies include wireless sensor network, positioning technology, and location-based services.

**LIN MA** (Member, IEEE) received the B.S., M.S., and Ph.D. degrees from the Harbin Institute of Technology (HIT), Harbin, China, in 2003, 2005, and 2009, respectively, all in communication engineering. From 2013 to 2014, he was a Visiting Scholar with the Edward S. Rogers, Sr. Department of Electrical and Computer Engineering, University of Toronto, Canada. He is currently an Associate Professor with the School of Electronics and Information Engineering, HIT. His current research interests include location-based service, cognitive radio, and cellular networks.

**XINXIN WANG** received the bachelor's degree in communication engineering from Qiqihar University, in 2018. She is currently a Postgraduate Fellow with the School of Electronics Engineering, Heilongjiang University. She has been a member of the Advance Ubiquitous Networking Communication Team. Her current research interests include the key technologies include wireless sensor networks, positioning technology, and location-based services.

**TEKLU MERHAWIT BERHANE** received the B.Sc. degree in electrical engineering from Bahirdar University, Bahir Dar, Ethiopia, in 2007, the M.Sc. degree in communication engineering from the Addis Ababa Institute of Technology, Addis Ababa, Ethiopia, in 2011, and the Ph.D. degree from the Harbin Institute of Technology (HIT), Harbin, China, in 2014. She is currently working with the School of Electrical and Computer Engineering, Dire Dawa University (DDU), Dire Dawa, Ethiopia. Her current research interests include spectral efficiency, energy balance, and communication systems design for WSN.

• • •